

## A Cell-less BEM Formulation for 2D and 3D Elastoplastic Problems Using Particular Integrals

A. Owatsiriwong<sup>1</sup>, B. Phansri<sup>1</sup> and K.H. Park<sup>1,2</sup>

**Abstract:** This study deals with the particular integral formulation for two (2D) and three (3D) dimensional elastoplastic analyses. The elastostatic equation is used for the complementary solution. The particular integrals for displacement, stress and traction rates are derived by introducing the concept of global shape function to approximate an initial stress rate term of the inhomogeneous equation. The Newton-Raphson algorithm for the plastic multiplier is used to solve the system equation. The developed program is integrated with the pre- and post-processor. The collapse analyses of the smooth flexible strip, square and circular footings are given by comparing the numerical results of the load-displacement response with those by other BEM and FEM programs. The results of evolution of plastic region and deformed shape with increasing load are also given to demonstrate the application and accuracy of the present formulation.

**Keyword:** BEM, particular integrals, elastoplasticity, Newton-Raphson algorithm, collapse analysis, footing.

### 1 Introduction

The boundary element method (BEM) has developed into a powerful numerical method for solving elastoplastic problems. Since Swedlow and Cruse (1971) had presented the first elastoplastic BEM formulation by incorporating a volume integral involving plastic strains, the elastoplastic BEM formulations have been developed into two main approaches: the initial stress ap-

proach [Banerjee et al. (1979), Cathie and Banerjee (1980), Banerjee and Raveendra (1986, 1987), Chopra and Dargush (1994), Gao and Davies (2002), Wang et al. (2007)] and the initial strain approach [Kumar and Mukherjee (1977), Telles and Brebbia (1979), Mukherjee (1982), Telles (1983), Chandra and Saigal (1991), Bonnet and Mukherjee (1996), Chandra and Mukherjee (1996), Poon et al. (1996), Benallal et al. (2002), Mallardo and Alessandri (2004)]. The large deformation algorithms have been also developed [Okada et al. (1989, 1990), Chandra and Saigal (1991), Okada and Atluri (1992a,b, 1994)]. However, these formulations are not a boundary-only formulation, and the volume cells are necessary for the body where plasticity is expected to develop. Few attempts have been made to eliminate this volume integration problem in elastoplastic analyses by using two methods: the volume integral conversion method and the particular integral method.

For conservative systems of body forces, such as a steady-state temperature, centrifugal acceleration, seepage gradient and gravitational potential, the exact forms of volume integral conversion method can be obtained [Cruse (1975), Rizzo and Shippy (1977), Cruse et al. (1977), Banerjee and Butterfield (1981), Danson (1981)]. However, for certain situations these body forces cannot be expressed analytically. In order to overcome this problem, Nardini and Brebbia (1982) introduced a radial basis function for free vibration analysis and later called this method the dual reciprocity method mainly because the resulting volume integral is converted to an equivalent pair of surface integrals giving the appearance of the use of a double reciprocal theorem [Nardini and Brebbia (1986)]. Recently, Ochiai and Kobayashi (1999) presented an improved multiple

<sup>1</sup> School of Engineering & Technology, Asian Institute of Technology, P.O. Box 4, Klong Luang, Pathumthani 12120, Thailand

<sup>2</sup> Corresponding author. Tel.: 66-2-524-5508; Fax: 66-2-524-5509. E-mail: khpark@ait.ac.th

reciprocity method for elastoplastic analysis with 2D numerical examples of a thick cylinder and a perforated plate. Gao (2002) also proposed a technique, named in the radial integral method, for elastoplastic problems. In this method, a strongly singular domain integral in internal stress integral equations was analytically transformed to the boundary, whereas other weakly singular domain integrals were transformed to the boundary by using the dual reciprocity method with different radial basis functions. One application of a 3D flexible square footing was given by comparing the result of load-settlement response with those by the cell-integration method. The method has been also applied to several engineering problems [Albuquerque and Aliabadi (2008), Tsai (2008), Dziatkiewicz and Fedelinski (2007), Davies et al. (2007), Fedelinski and Gorski (2006), Cho et al. (2004), Wen et al. (2002), Ochiai (2001), Kogl and Gaul (2000)].

The particular integral method is a classical technique, obtaining the total solution as the sum of a complementary solution for the homogeneous part of the differential equation and a particular solution for the total governing inhomogeneous differential equation. Because of its simplicity and well established mathematical roots, the method has been recently extended to several engineering problems [Owatsiriwong and Park (2008), Park and Banerjee (2002a,b, 2006, 2007), Park (2002, 2003), Yang et al. (2002)].

There has been some confusion between the particular integral method and dual reciprocity method. Polyzos et al. (1994) stated two methods are formally equivalent, while Power and Partridge (1994) stated that for the case in which the non-homogeneous term is a known function, the particular integral method is numerically more efficient, but for the case in which the non-homogeneous term is an unknown function both methods are numerically equivalent. Although the fundamental mathematical bases of two methods are different, some of these confusions have mainly occurred due to the superficial similarities of the matrix algebra involved. For more details on the comparison of both the particular integral method and volume integral conversion method

the reader may see Yang et al. (2002).

In fact, Henry and Banerjee (1988) presented the particular integral formulation for elastoplastic problems in 1988. They showed 2D and 3D numerical examples, such as 3D analyses of a cube, a notch plate and a perforated plate, and 2D analysis of a perforated plate, and compared the numerical results of the stress-strain response for different nonlinear system equation solution algorithms (iterative and variable stiffness). However, the Newton-Raphson algorithm is now popular for solving sets of nonlinear equations in BEM [Chopra and Dargush (1994), Bonnet and Mukherjee (1996), Poon et al. (1996), Gao and Davies (2002), Benallal et al. (2002), Mallardo and Alessandri (2004), Wang et al. (2007)]. It is necessary to demonstrate the potential of the method by giving strong benchmark tests and engineering applications and using the advanced solution algorithm.

This study addresses this issue for the particular integral formulation of 2D and 3D elastoplastic analyses. First the detailed explanation for the derivation of the formulation and numerical implementation is given. The solution of the elastostatic equation is used as the complementary solution. A global shape function is considered to approximate the initial stress rate term of the inhomogeneous equation so that the particular integrals for displacement, stress and traction rates are derived for 2D and 3D formulations. The Newton-Raphson algorithm for the plastic multiplier is used to solve the system equation. The GiD software package (2007) is used as the pre- and post-processing tool. For benchmark tests, the first three examples, such as a cube under uniaxial tension, a thick-walled cylinder under internal pressure and a thick-walled hollow sphere under internal pressure, are given and the accuracy of the present formulation are shown by comparing the numerical results with analytical solutions. Then the collapse analyses of the smooth flexible strip, square and circular footings are given to demonstrate the application to geomechanics problem. Numerical results of the load-displacement response at typical location are compared with those by other volume integra-

tion BEM programs and finite element software ABAQUS (2004). The results of evolution of plastic region and deformed shape with increasing load are given to show the application and accuracy of the present formulation.

## 2 Particular integral formulation

The governing differential equation for incremental elastoplasticity of a homogeneous and isotropic body can be expressed in terms of incremental displacement  $\dot{u}_i$  as [Banerjee (1994), Henry and Banerjee (1988)]

$$(\lambda + \mu)\dot{u}_{j,ji} + \mu\dot{u}_{i,jj} = \dot{\sigma}_{ij,j}^o \quad (1)$$

where  $\lambda$  and  $\mu$  are Lamé's constants,  $\dot{\sigma}_{ij}^o$  is the initial stress rate resulting from the non-linearities present in the plastic domain, a superior dot denotes an increment, commas represent differentiation with respect to spatial coordinates, and  $i, j=1,2(3)$  for two(three) dimensions. The incremental initial stress rate is defined as

$$\dot{\sigma}_{ij}^o = \dot{\sigma}_{ij}^e - \dot{\sigma}_{ij}^{ep} \quad (2)$$

where  $\dot{\sigma}_{ij}^e = D_{ijkl}^e \dot{\epsilon}_{kl}$ ,  $\dot{\sigma}_{ij}^{ep} = D_{ijkl}^{ep} \dot{\epsilon}_{kl}$ ,  $\dot{\epsilon}_{kl}$  is the strain rate and  $D_{ijkl}^e$ ,  $D_{ijkl}^{ep}$  are the elastic and elastoplastic constitutive tensors respectively.

The solution of Eq.1 can be represented as a sum of complementary function  $\dot{u}_i^c$  satisfying the homogeneous equation

$$(\lambda + \mu)\dot{u}_{j,ji}^c + \mu\dot{u}_{i,jj}^c = 0 \quad (3)$$

and particular integral  $\dot{u}_i^p$  satisfying the inhomogeneous equation

$$(\lambda + \mu)\dot{u}_{j,ji}^p + \mu\dot{u}_{i,jj}^p = \dot{\sigma}_{ij,j}^o \quad (4)$$

where superscripts  $c$  and  $p$  indicate complementary and particular solutions respectively.

Then the total solutions for displacement rate  $\dot{u}_i$ , stress rate  $\dot{\sigma}_{ij}$ , and traction rate  $\dot{t}_i$  can be obtained as

$$\dot{u}_i = \dot{u}_i^c + \dot{u}_i^p \quad (5a)$$

$$\dot{\sigma}_{ij} = \dot{\sigma}_{ij}^c + \dot{\sigma}_{ij}^p \quad (5b)$$

$$\dot{t}_i = \dot{t}_i^c + \dot{t}_i^p \quad (5c)$$

where  $\dot{\sigma}_{ij}^c$ ,  $\dot{t}_i^c$  and  $\dot{\sigma}_{ij}^p$ ,  $\dot{t}_i^p$  are the complementary functions and particular integrals for stress and traction rates, respectively.

## 2.1 Complementary solutions

The boundary integral equation related to the complementary functions  $u_i^c$  and  $t_i^c$  can be written as [Banerjee (1994)]

$$C_{ij}(\xi)\dot{u}_i^c(\xi) = \int_S [G_{ij}(x, \xi)\dot{t}_i^c(x) - F_{ij}(x, \xi)\dot{u}_i^c(x)] dS(x) \quad (6)$$

where  $G_{ij}$  and  $F_{ij}$  are the fundamental solutions for elastostatic equation (for details see Banerjee (1994), pg.96-97) and  $C_{ij}(\xi) = 1, 0$  and  $1/2$  depending on the point  $\xi$  being in the interior, outside or on a smooth boundary point respectively.

The complementary function for the interior stress rate  $\dot{\sigma}_{ij}^c$  can be written by using the stress-strain relationship as [Banerjee (1994)]

$$\dot{\sigma}_{ij}^c(\xi) = \int_S [G_{kij}^\sigma(x, \xi)\dot{t}_k^c(x) - F_{kij}^\sigma(x, \xi)\dot{u}_k^c(x)] dS(x) \quad (7)$$

where  $G_{kij}^\sigma$  and  $F_{kij}^\sigma$  are the kernel functions for stresses (for details see Banerjee (1994), pg.100-101).

## 2.2 Particular integrals

The standard direct BEM formulation for Eq.1 using the elastostatic fundamental solution of Eq.3 will unfortunately contain the unknown initial stress rate  $\dot{\sigma}_{ij}^o(x)$  as integrals within domain. However, by using the Galerkin vector and approximating the initial stress rate term with known global shape function, an attempt can be made to convert the volume integral into a surface integral [Henry and Banerjee (1988)].

By using Galerkin vector  $F_i$  [Fung (1965)], the particular integral for displacement rate  $\dot{u}_i^p$  can be expressed as

$$\dot{u}_i^p(x) = \frac{1-\nu}{\mu} \dot{F}_{i,kk}(x) - \frac{1}{2\mu} \dot{F}_{k,ki}(x) \quad (8)$$

where  $\nu$  is the Poisson's ratio.

Substituting of Eq.8 into Eq.4 yields

$$\dot{F}_{i,lljj} = \frac{1}{1-\nu} \dot{\sigma}_{ij,j}^o \quad (9)$$

Considering the implicit expression of Eq.8 and Eq.9 to be related by a second order tensor  $\dot{h}_{ij}$ , rather than a vector, one can introduce the following relation:

$$\dot{h}_{ij,kknn} = \dot{\sigma}_{ij}^o \quad (10)$$

Substitution of this equation into Eq.9 yields an expression for the Galerkin vector in terms of this new function:

$$\dot{F}_i = \frac{1}{1-\nu} \dot{h}_{ij,j} \quad (11)$$

Then substituting this expression into Eq.8 yields the desired particular integral for displacement rate

$$\dot{u}_i^p = \frac{1}{\mu} \dot{h}_{il,lkk} - \frac{1}{2\mu(1-\nu)} \dot{h}_{lm,ilm} \quad (12)$$

By introducing the global shape function  $C(x, \xi_n)$ , the initial stress rate  $\dot{\sigma}_{ij}^o(x)$  can be approximated as

$$\dot{\sigma}_{ml}^o(x) = \sum_{n=1}^{\infty} C(x, \xi_n) \dot{\phi}_{ml}(\xi_n) \quad (13)$$

where  $\dot{\phi}_{ml}(\xi_n)$  is the unknown fictitious function.

Assuming

$$\dot{h}_{ml}(x) = \sum_{n=1}^{\infty} H(x, \xi_n) \dot{\phi}_{ml}(\xi_n) \quad (14)$$

and substituting Eq.13 and Eq.14 into Eq.10 one can obtain

$$H_{,kknn} = C \quad (15)$$

Since the global shape function is used to approximate  $\dot{\sigma}_{ij}^o(x)$ , the choice of these functions has direct effect on the accuracy of the method. However, the choice of complementary and particular solutions is somewhat arbitrary because it is the total solution which provides the uniqueness of the solution by satisfying the boundary conditions. More elaborate global shape functions may have better modeling capabilities on their own but used in the context of particular integrals may not show any better performance. Because of this

fact, the following simple and efficient function is chosen here:

$$C(x, \xi_n) = A - r \quad (16)$$

with

$$H(x, \xi_n) = (H_1 A - H_2 r) r^4 \quad (17)$$

where  $H_1$  and  $H_2$  are constants,  $r^2 = y_i y_i$ ,  $y_i = [x_i - (\xi_n)_i]$  and  $A$  is a constant chosen as the largest distance between  $x$  and  $\xi_n$ .

By substituting Eq.16 and Eq.17 into Eq.15, the coefficients  $H_1$  and  $H_2$  can be derived as

$$H_1 = \frac{1}{8d(d+2)}; \quad H_2 = \frac{1}{15(d+3)(d+1)} \quad (18)$$

where  $d$  is the dimension, that is  $d=2$  for 2D or  $d=3$  for 3D analysis.

Then the particular integral for displacement rate can be derived as

$$\dot{u}_i^p(x) = \sum_{n=1}^{\infty} U_{iml}(x, \xi_n) \dot{\phi}_{ml}(\xi_n) \quad (19)$$

where

$$\begin{aligned} U_{iml}(x, \xi_n) &= \frac{1}{\mu} \delta_{im} \frac{\partial^3 H}{\partial x_l \partial x_k \partial x_k} - \frac{1}{2\mu(1-\nu)} \frac{\partial^3 H}{\partial x_i \partial x_l \partial x_m} \\ &= (U_1 A + U_2 r) (\delta_{lm} y_i + \delta_{il} y_m) + (U_3 A + U_4 r) \delta_{im} y_l \\ &\quad + \frac{U_2}{r} y_i y_l y_m \end{aligned} \quad (20)$$

$$U_1 = -\frac{8H_1}{2\mu(1-\nu)}; \quad U_2 = \frac{15H_2}{2\mu(1-\nu)} \quad (21)$$

$$U_3 = U_1 + \frac{8(2+d)H_1}{\mu}; \quad U_4 = U_2 - \frac{15(3+d)H_2}{\mu} \quad (22)$$

A particular integral for stress rate can be derived by substituting Eq.19 and Eq.20 into the strain-displacement relation and the stress-strain law:

$$\dot{\sigma}_{ij}^p(x) = \sum_{n=1}^{\infty} S_{ijml}(x, \xi_n) \dot{\phi}_{ml}(\xi_n) \quad (23)$$

where

$$\begin{aligned}
& S_{ijml}(x, \xi_n) \\
& = (e_2A + f_2r)\delta_{jm}\delta_{il} + (e_3A + f_3r)\delta_{ij}\delta_{lm} \\
& \quad + (e_4A + f_4r)\delta_{im}\delta_{jl} \\
& \quad + \frac{f_1}{r}(\delta_{il}y_jy_m + \delta_{lm}y_iy_j + \delta_{jl}y_iy_m) \\
& \quad + \frac{f_2}{r}(\delta_{jm}y_iy_l + \delta_{im}y_jy_l) + \frac{f_3}{r}\delta_{ij}y_ly_m \\
& \quad + \frac{f_5}{r^3}y_iy_jy_ly_m
\end{aligned} \tag{24}$$

$$\begin{aligned}
e_1 & = 2\mu U_1; \quad e_2 = \mu(U_1 + U_3); \\
e_3 & = e_1 + \lambda\{U_1(1+d) + U_3\}; \\
e_4 & = e_2 - 1
\end{aligned} \tag{25}$$

$$\begin{aligned}
f_1 & = -f_5 = 2\mu U_2; \quad f_2 = \mu(U_2 + U_4); \\
f_3 & = f_1 + \lambda\{U_2(2+d) + U_4\}; \\
f_4 & = f_2 + 1
\end{aligned} \tag{26}$$

Then a particular integral for traction rate is derived by multiplying the above equation with the appropriate normals:

$$i_i^p(x) = \sum_{n=1}^{\infty} T_{iml}(x, \xi_n) \dot{\phi}_{ml}(\xi_n) \tag{27}$$

where

$$T_{iml}(x, \xi_n) = S_{ijml}(x, \xi_n) n_j \tag{28}$$

$n_j(x)$  = unit normal at  $x$  in the  $j$ -th direction.

### 3 Numerical implementation

#### 3.1 Formulation of the system equation

The boundary integral Eq.6 and stress Eq.7 can be written in matrix form as [Banerjee (1994)]

$$[G_{ij}] \{t_i^c\} - [F_{ij}] \{u_i^c\} = 0 \tag{29}$$

$$\{\dot{\sigma}_{ij}^c\} = [G_{kij}^{\sigma}] \{t_k^c\} - [F_{kij}^{\sigma}] \{u_k^c\} \tag{30}$$

Considering the total solutions of Eq.5 the complementary functions in Eq.29 and Eq.30 can be eliminated as

$$[G_{ij}] \{t_i\} - [F_{ij}] \{u_i\} = [G_{ij}] \{t_i^p\} - [F_{ij}] \{u_i^p\} \tag{31}$$

$$\begin{aligned}
\{\dot{\sigma}_{ij}\} & = [G_{kij}^{\sigma}] \{t_k\} - [F_{kij}^{\sigma}] \{u_k\} - [G_{kij}^{\sigma}] \{t_k^p\} \\
& \quad - [F_{kij}^{\sigma}] \{u_k^p\} + \{\dot{\sigma}_{ij}^p\}
\end{aligned} \tag{32}$$

If a finite number of  $\xi_n$ ,  $N$ , are chosen, the particular integrals for displacement, traction and stress rates can be written as

$$\{\dot{u}_i^p\} = [U_{iml}] \{\dot{\phi}_{ml}\} \tag{33}$$

$$\{t_i^p\} = [T_{iml}] \{\dot{\phi}_{ml}\} \tag{34}$$

$$\{\dot{\sigma}_{ij}^p\} = [S_{ijml}] \{\dot{\phi}_{ml}\} \tag{35}$$

Considering the fictitious nodal values as

$$\{\dot{\phi}_{ml}\} = [C]^{-1} \{\dot{\sigma}_{ml}^o\} \tag{36}$$

Eq.31 and Eq.32 becomes

$$[G_{ij}] \{t_i\} - [F_{ij}] \{u_i\} = [M_{jml}^b] \{\dot{\sigma}_{ml}^o\} \tag{37}$$

$$\{\dot{\sigma}_{ij}\} = [G_{kij}^{\sigma}] \{t_k\} - [F_{kij}^{\sigma}] \{u_k\} - [M_{ijml}^{\sigma}] \{\dot{\sigma}_{ml}^o\} \tag{38}$$

where

$$[M_{jml}^b] = ([G_{ij}] [T_{iml}] - [F_{ij}] [D_{iml}]) [C]^{-1} \tag{39}$$

$$\begin{aligned}
[M_{ijml}^{\sigma}] & = \\
& \left( [G_{kij}^{\sigma}] [T_{kml}] - [F_{kij}^{\sigma}] [D_{kml}] - [S_{ijml}] \right) [C]^{-1}
\end{aligned} \tag{40}$$

Then the final system of equations can be obtained as

$$[A^b] \{\dot{x}\} = \{y^b\} - [M^b] \{\dot{\sigma}^o\} \tag{41}$$

$$\{\dot{\sigma}\} = \{y^{\sigma}\} + [A^{\sigma}] \{\dot{x}\} - [M^{\sigma}] \{\dot{\sigma}^o\} \tag{42}$$

where  $A^b$ ,  $M^b$ ,  $A^{\sigma}$  and  $M^{\sigma}$  are block-banded matrices,  $\dot{x}$  is a vector of unknown boundary quantities,  $y^b$  and  $y^{\sigma}$  are vectors of known boundary conditions,  $\dot{\sigma}$  is a vector of stress rate, and  $\dot{\sigma}^o$  is a vector of initial stress rates at the boundary and interior points. Eq.41 and Eq.42 are nonlinear system due to the unknown initial stress vector  $\sigma^o$ . In this study, the Newton-Raphson algorithm for the plastic multiplier is employed for elastoplastic solution.

### 3.2 Newton-Raphson algorithm with plastic multiplier

The detailed explanation for the Newton-Raphson algorithm and the corresponding computer program can be found in the reference [Gao and Davies (2002)]. Here the brief explanation is given for completeness.

The elastic stress increment can be decomposed into the total (or correct) stresses and the initial stresses via

$$\{\dot{\sigma}^e\} = \{\dot{\sigma}\} + \{\dot{\sigma}^o\} \quad (43)$$

Using Eq.42 for total stress and the plastic multiplier  $\lambda$  [Gao and Davies (2002)],

$$\{\dot{\lambda}\} = \{\nabla f_{\psi}\}^T \{\dot{\sigma}^e\} \quad (44)$$

Eq.43 can be rewritten as

$$[A^{\lambda}] \{\dot{\lambda}\} = \{\dot{y}^f\} \quad (45)$$

where

$$[A^{\lambda}] = [I] - [\nabla f_{\psi}] \left( [I] - [A^{\sigma}] [A^b]^{-1} [M^b] - [M^{\sigma}] \right) [d^f] \quad (46)$$

$$\{\dot{y}^f\} = [\nabla f_{\psi}] \left( \{\dot{y}^{\sigma}\} + [A^{\sigma}] [A^b]^{-1} \{\dot{y}^b\} \right) \quad (47)$$

$$\{\nabla f_{\psi}\} = \frac{1}{\psi} \left\{ \frac{\partial f}{\partial \sigma} \right\} \quad (48)$$

$$\psi = \left\{ \frac{\partial f}{\partial \sigma} \right\} [D^e] \left\{ \frac{\partial f}{\partial \sigma} \right\} + H^* \left\{ \frac{\partial h^{\alpha}}{\partial \lambda} \right\} \quad (49)$$

$$\{d^f\} = [D^e] \left\{ \frac{\partial f}{\partial \sigma} \right\} \quad (50)$$

$f$  is the yield function,  $H^*$  is the weighted average of the isotropic and kinematic hardening parameters and  $h^{\alpha}$  is the internal variable.

Then the residual of Eq.45, following the  $i$ -th iteration,  $R^i$  can be written as

$$\{R\}^i = \{\dot{y}^f\}^i - [A^{\lambda}]^i \{\dot{\lambda}\}^i \quad (51)$$

By using Taylor's series expansion, the incremental change of plastic multiplier  $\Delta\dot{\lambda}$  can be obtained as

$$[A^{\lambda}]^i \{\Delta\dot{\lambda}\} = \{R\}^i \quad (52)$$

Also the corresponding changes in boundary unknowns and stress can be obtained as

$$\{\Delta\dot{x}\} = -[A^b]^{-1} [M^b] [d^f] \{\Delta\dot{\lambda}\} \quad (53)$$

$$\{\Delta\dot{\sigma}\} = - \left( [A^{\sigma}] [A^b]^{-1} [M^b] + [M^{\sigma}] \right) [d^f] \{\Delta\dot{\lambda}\} \quad (54)$$

Then the variables are updated by

$$\{\dot{\lambda}\}^{i+1} = \{\dot{\lambda}\}^i + \{\Delta\dot{\lambda}\} \quad (55)$$

$$\{\dot{x}\}^{i+1} = \{\dot{x}\}^i + \{\Delta\dot{x}\} \quad (56)$$

$$\{\dot{\sigma}\}^{i+1} = \{\dot{\sigma}\}^i + \{\Delta\dot{\sigma}\} \quad (57)$$

### 3.3 Calculation sequence

The computation can be summarized as follows:

- (1) Solve the elastic problem in the usual manner. Scale the elastic solution such that the most highly stress node is at yield. Store the current values of stresses.
- (2) Apply small load increment  $\{\dot{y}^b\}, \{\dot{y}^{\sigma}\}$ .
- (3) Scale stresses for each node.
- (4) Initialize iterative variables for each node.
- (5) Obtain  $\{\Delta\dot{\lambda}\}$  in Eq.52, and then update  $\{\dot{\lambda}\}^{i+1}, \{\dot{x}\}^{i+1}$  and  $\{\dot{\sigma}\}^{i+1}$  in Eq.55~Eq.57.
- (6) If the solution of  $\Delta\dot{\lambda}$  does not converge, go to step (5) for the next iteration step.
- (7) If converge, update unknown variables and internal variables and go to step (2) for the next load increment.

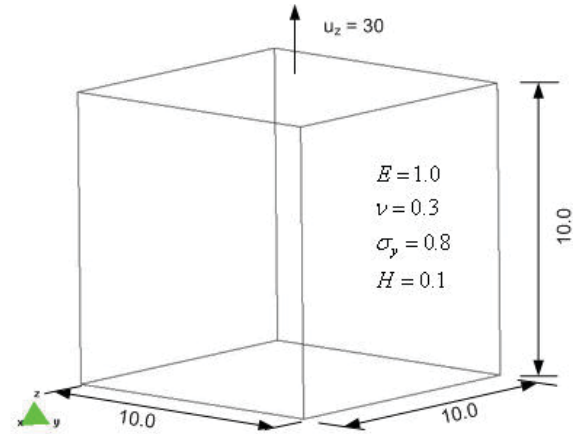
## 4 Numerical applications

In order to show the validity and accuracy of the present formulation, six examples of application are given. The results of the load-displacement response at typical location are compared with their analytical solutions and those by other volume integration BEM programs, such as GPBEST [Wang et al. (2007), Chatterjee (2002)], BEMECH [Gao and Davies (2002)], and finite element software ABAQUS (2004). The same modeling meshes are used for comparison of the results in ABAQUS, BEMECH, and TS (this study). The results of evolution of plastic region and the corresponding deformed shape with increasing load are also given. While the present program can be used for the different material models, such as Tresca, von Mises, Mohr-Coulomb and Drucker-Prager models, the examples consider the von Mises model only.

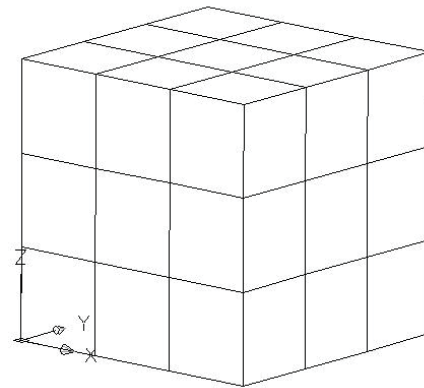
### 4.1 Example 1: cube under uniaxial tension

The first example deals with a 10-unit cube subjected to nodal displacement (Fig. 1(a)) [Gao and Davies (2002)]. The displacement of 30-unit is prescribed at the top surface, while other surfaces are restrained against normal displacement by using roller boundary condition for symmetric boundary condition about 3 planes (ZX, XY, YZ). Typical modeling mesh using 54 quadratic boundary elements for 3D analysis is shown in Fig. 1(b). In order to show the influence of interior points to the solution accuracy, two cases are considered: one with 44 interior points and the other without interior point. The values of material properties used are:  $E=1.0$ ,  $\nu=0.3$ ,  $\sigma_y=0.8$  and  $H=0.1$ , where  $E$  is the modulus of elasticity,  $\sigma_y$  is the Mises equivalent uniaxial yield strength, and  $H$  is the isotropic hardening modulus.

Numerical results for load-displacement response at the top surface are compared with analytical solution (A.S.), as shown in Fig. 2. Good agreement can be seen for both models where the mesh including interior points yields better accuracy in this case. Since the stress field remains constant (Fig. 3), very small discrepancy of analysis results is noticed between the models with and with-



(a) Problem statement



(b) 3D modeling mesh

Figure 1: A cube subjected to uniaxial prescribed displacement (Example 1)

out interior points. For the problem with complex stress field, this is not the case.

### 4.2 Example 2: thick-walled cylinder under internal pressure

A thick-walled cylinder subjected to internal pressure is analyzed as the second example problem (Fig. 4). The inner radius  $a=100.0$  and outer radius  $b=200.0$ . The 2D modeling mesh, as shown in Fig. 4(a), uses 32 quadratic boundary elements and 161 interior points, while Fig. 4(b) shows 3D modeling mesh using 96 quadratic boundary elements and 25 interior points. For 2D and 3D analyses only the positive octant of the cylinder is modeled, while symmetric constraints are im-

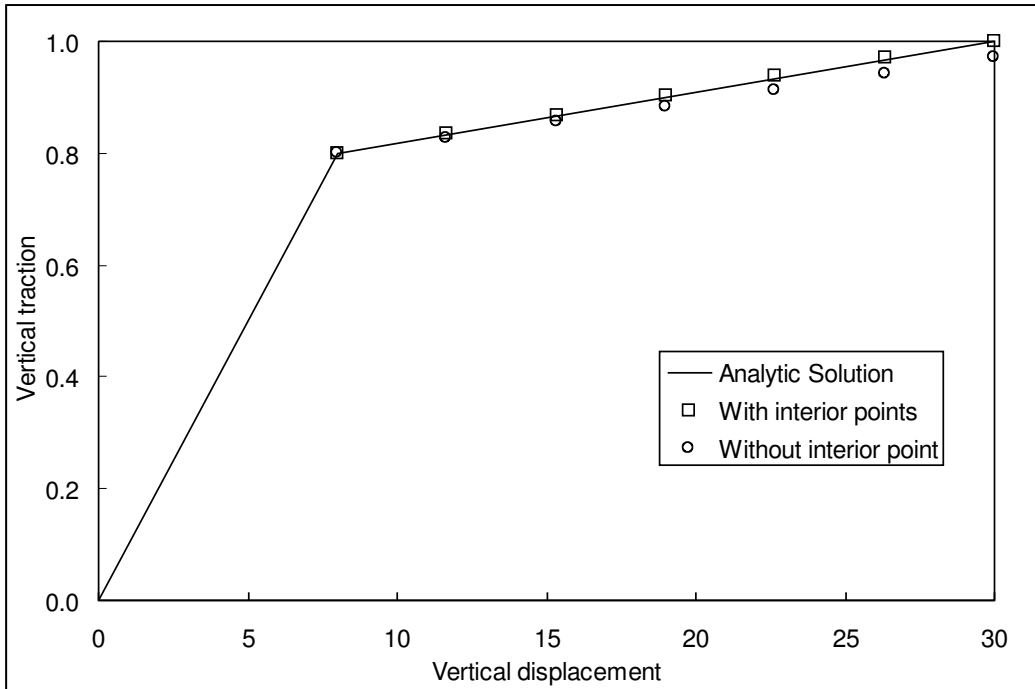


Figure 2: Load-displacement response (Example 1)

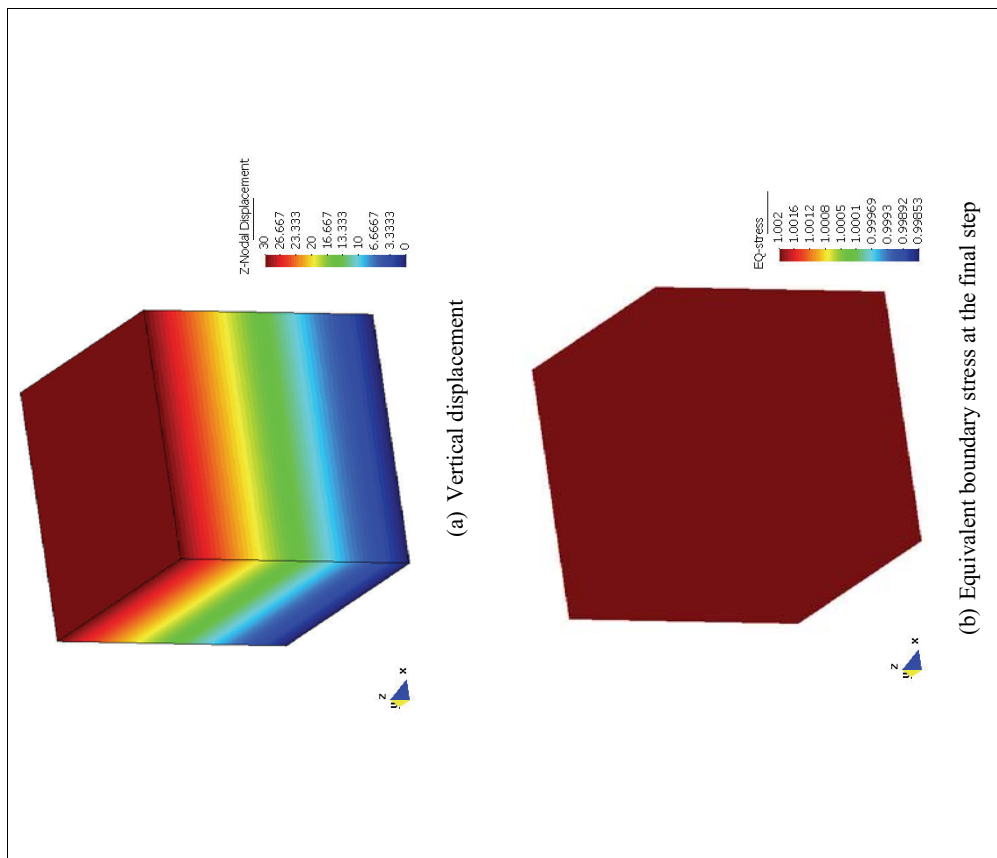


Figure 3: Contour plots of the results (Example 1)

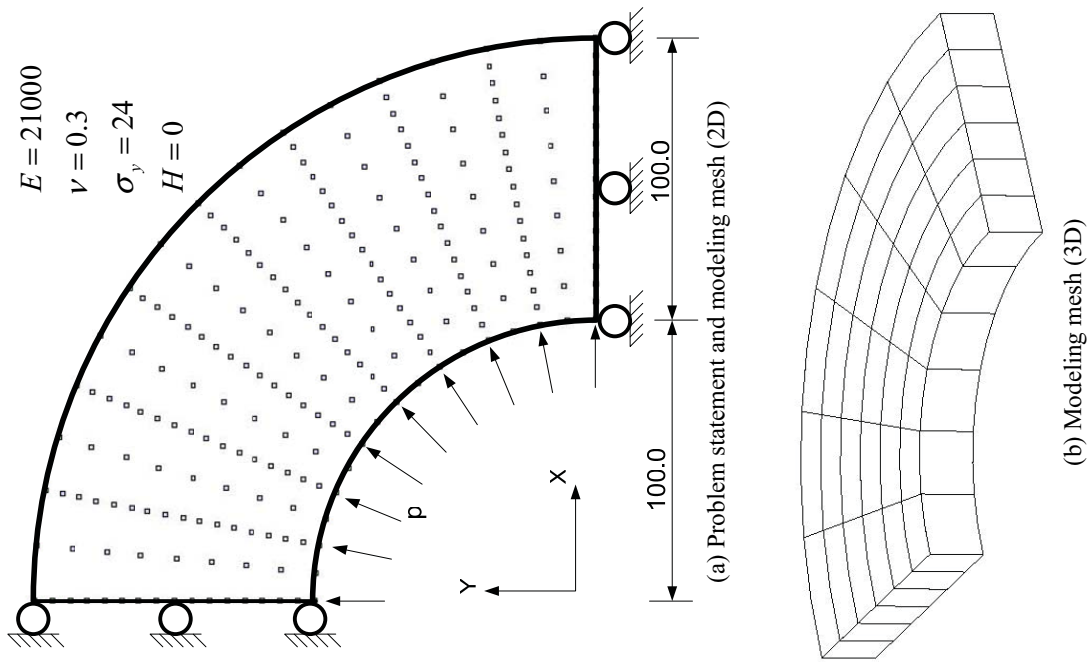


Figure 4: A thick-walled cylinder subjected to internal pressure (Example 2)

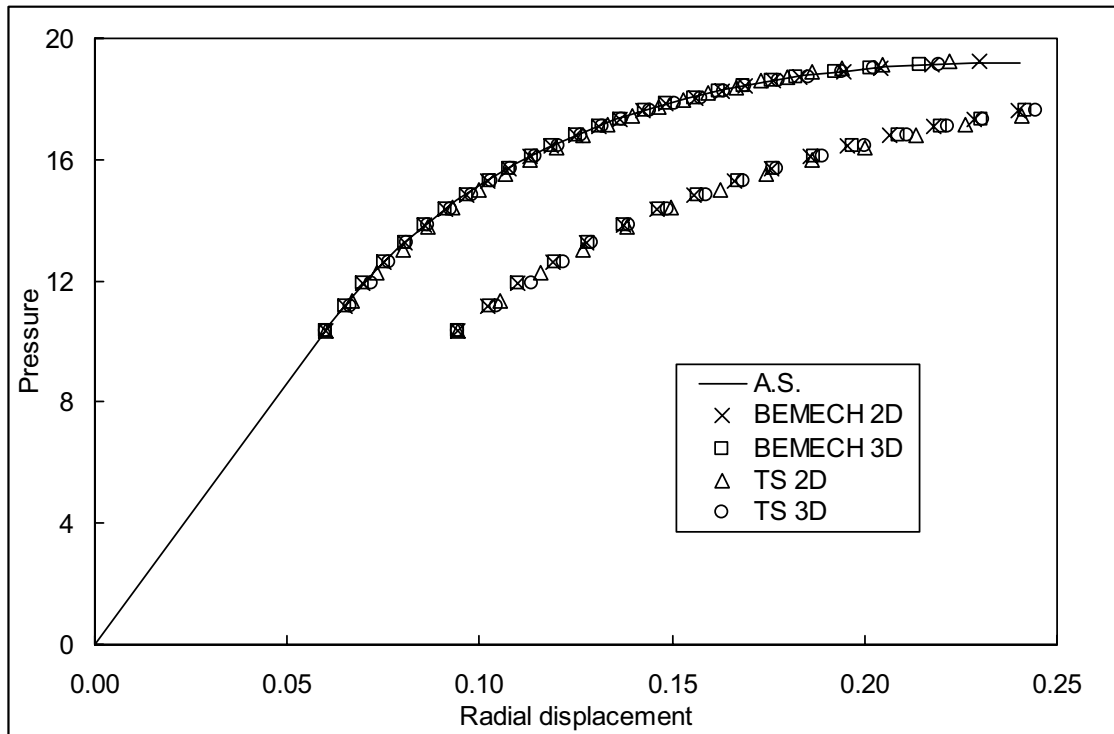
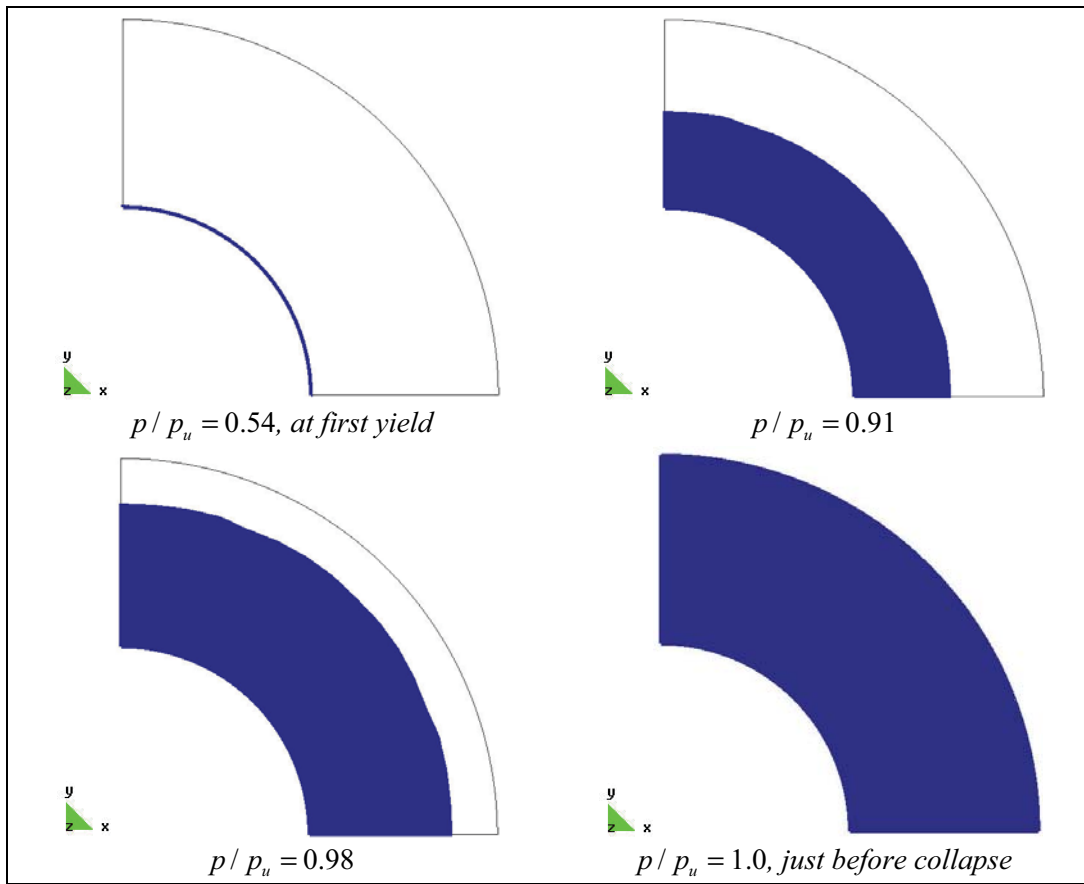
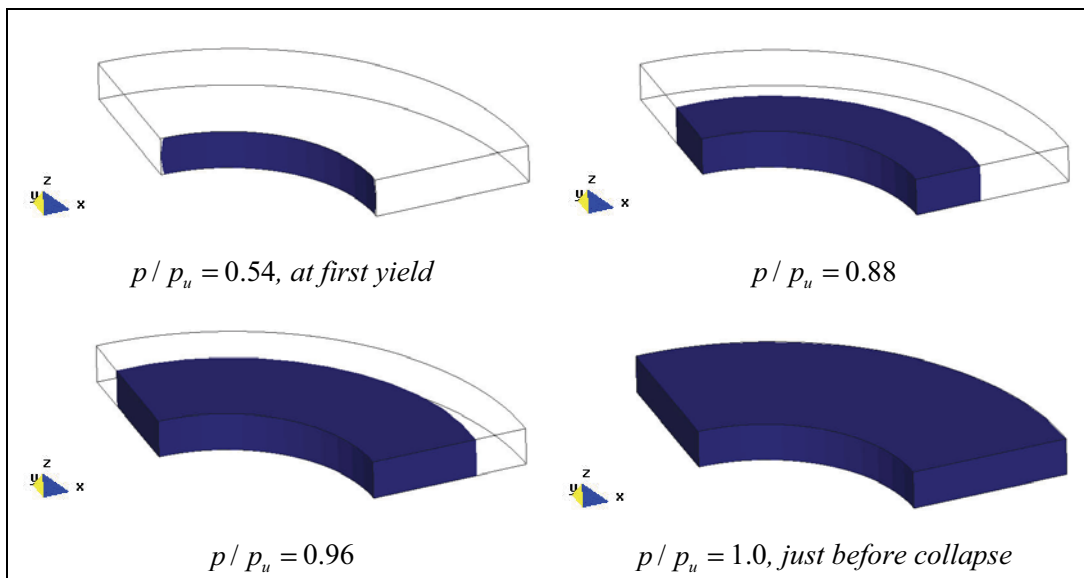


Figure 5: Load-displacement response (Example 2)



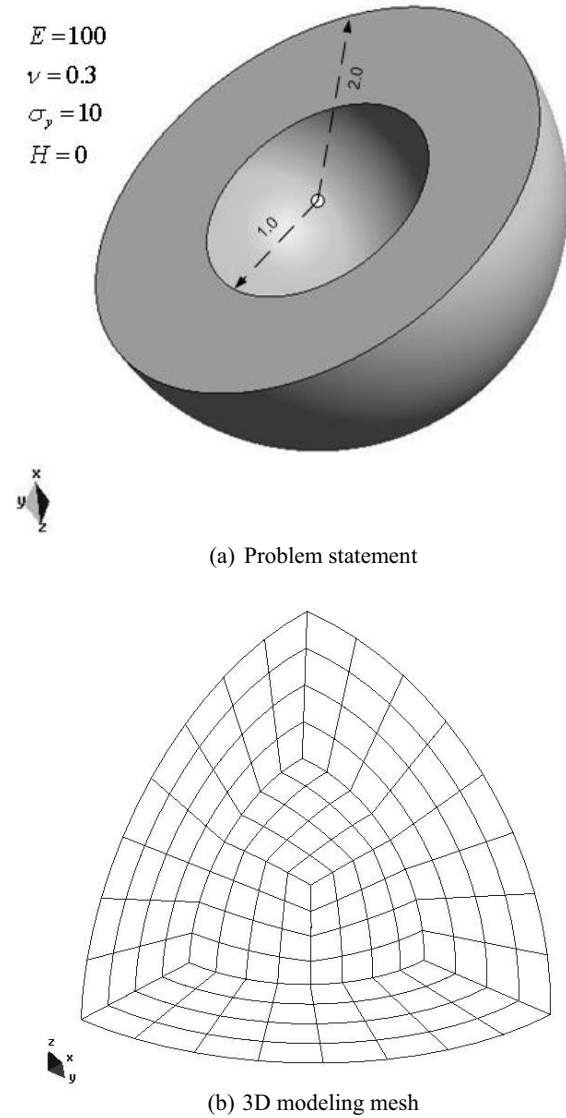
(a) 2D



(b) 3D

Figure 6: Evolution of plastic region (Example 2)

posed.



(a) Problem statement

(b) 3D modeling mesh

Figure 7: A thick-walled hollow sphere subjected to internal pressure (Example 3)

The analytical solution for the displacement at the outer surface can be obtained for the von Mises' yield criterion [Hill (1950), pg. 108~118]

$$u_o(b) = \frac{2(1-\nu^2)}{E \left( \frac{b^2}{a^2} - 1 \right)} p_o b$$

with

$$p_o = \frac{\frac{\sigma_y}{\sqrt{3}} \left( 1 - \frac{a^2}{b^2} \right)}{\sqrt{\left\{ 1 + (1-2\nu)^2 \frac{a^4}{3b^4} \right\}}}$$

for initial yielding

$$u(b) = \frac{2(1-\nu^2)}{\sqrt{3}Eb} \sigma_y c^2$$

after initial yielding where  $c$  is the radius of the plastic boundary and found to be

$$p = \frac{1}{\sqrt{3}} \sigma_y \left\{ 1 - \frac{c^2}{b^2} + \ln \frac{c^2}{a^2} \right\}.$$

The load-displacement response at the inner and outer surfaces is compared with the analytical solution and that of BEMECH [Gao and Davies (2002)], as shown in Fig. 5. Good agreement can be seen for both 2D and 3D analyses. Fig. 6 shows the evolution of plastic region for both 2D and 3D meshes. Uniform expansion of the plastic region with increasing load confirms the accuracy of the present formulation.

### 4.3 Example 3: thick-walled hollow sphere under internal pressure

The third example is a thick-walled hollow sphere subjected to uniform internal pressure (Fig. 7(a)). The inner radius  $a=1.0$  and outer radius  $b=2.0$ . The typical modeling mesh for 3D analysis using 192 quadratic boundary elements and 511 interior points is shown in Fig. 7(b). Due to symmetry, a quarter of sphere is analyzed.

The analytical solutions for the displacement at the inner and outer surfaces can be obtained for the von Mises' criterion [Hill (1950), pg. 98~101]:

for initial yielding,

$$u_o(a) = \frac{\sigma_y a}{E} \left\{ \frac{2(1-2\nu)a^3}{3b^3} + \frac{1+\nu}{3} \right\},$$

$$u_o(b) = \frac{(1-\nu)}{Eb^2} \sigma_y a^3,$$

with

$$p_o = \frac{2}{3} \sigma_y \left( 1 - \frac{a^3}{b^3} \right)$$

after initial yielding,

$$u(a) =$$

$$\frac{\sigma_y a}{E} \left\{ (1-\nu) \frac{c^3}{a^3} - \frac{2}{3} (1-2\nu) \left( 1 - \frac{c^3}{b^3} + \ln \frac{c^3}{a^3} \right) \right\},$$

$$u(b) = \frac{(1-\nu)}{Eb^2} \sigma_y c^3$$

where  $c$  is found to be

$$p = \frac{2}{3}\sigma_y \left\{ 1 - \frac{c^3}{b^3} + \ln \frac{c^3}{a^3} \right\}.$$

The load-displacement response at the inner and outer surfaces is compared with the analytical solution and that of BEMECH [Gao and Davies (2002)], as shown in Fig. 8. Good agreement can be seen. Fig. 9 shows the evolution of plastic region with increasing load. Again, uniform expansion of the plastic region indicates the validity of the formulation.

#### 4.4 Example 4: collapse analysis of a flexible strip footing

The fourth example problem concerns a smooth flexible strip footing on an elastic-perfectly plastic half space, which has  $E = 20000$ ,  $\nu=0.49$  and  $\sigma_y = 173.21$  ( $c_u = \sigma_y/\sqrt{3} = 100$ ), where  $c_u$  is the undrained shear strength. The 2D modeling mesh using 38 quadratic boundary elements and 209 interior points is shown in Fig. 10(a), while the 3D modeling mesh uses 358 quadratic boundary elements and 126 interior points (Fig. 10(b)).

The non-dimensionalized load-displacement response at the center of the footing is shown in Fig. 11, together with the result obtained using the conventional volume integration and the mixed representation algorithm by GPBEST [Chatterjee (2002)] and ABAQUS (2004). The exact solution for the collapse load is well known and the collapse load in terms of undrained shear strength is  $(\pi + 2)c_u$ . The collapse loads obtained from the present analysis are  $5.07 c_u$  and  $5.04 c_u$  for 2D and 3D analyses respectively, indicating the acceptable accuracy of the analysis (discrepancy below 2% in both cases has been noticed). Fig. 12 shows the development of plastic region and the corresponding deformed shape (3 times magnified) for different load increment.

#### 4.5 Example 5: collapse analysis of a flexible square footing

The fifth example problem is the collapse analysis of a smooth flexible square footing on a homogeneous soil. The soil is assumed to be elastic-perfectly plastic obeying von Mises material with

the following properties:  $E = 1000$ ,  $\nu=0.3$  and  $\sigma_y = 17.321$  ( $c_u = \sigma_y/\sqrt{3} = 10$ ). Two different 3D modeling meshes, as shown in Fig. 13, are considered. The modeling mesh with four elements over footing uses 132 quadratic boundary elements and 220 interior points, as shown in Fig. 13(a), while 226 quadratic boundary elements and 600 interior points are used for nine elements over footing in Fig. 13(b).

The non-dimensionalized load-mean displacement response of the footing is shown in Fig. 14, together with the results by GPBEST [Chatterjee (2002)], BEMECH [Gao and Davies (2002)], and ABAQUS (2004). The mean displacement is obtained as  $u_m = (u_{corner} + 2u_{center})/3$  [Chatterjee (2002)]. In this case, the exact solution for the collapse load is not known, but the collapse load of a rigid circular footing, close to  $6 B^2 c_u$ , can be considered as a reference value. The collapse loads obtained from the present analysis are  $5.74 B^2 c_u$  and  $5.79 B^2 c_u$  for four and nine elements over footing respectively. Fig. 15 shows the evolution of plastic region and the corresponding deformed shape (2 times magnified) by the load increment. It can be seen that the plastic region extends laterally about two times and vertically slightly more than the footing dimensions.

#### 4.6 Example 6: collapse analysis of a flexible circular footing

The final example problem is the collapse analysis of a smooth flexible circular footing on a homogeneous soil. Again, the soil is assumed to be elastic-perfectly plastic obeying von Mises material with the same properties used in the previous example. Two different 3D modeling meshes are considered, as shown in Fig. 16. The modeling mesh with five elements over footing uses 104 quadratic boundary elements and 87 interior points, as shown in Fig. 16(a), while 216 elements and 470 interior points are used for twelve elements over footing in Fig. 16(b).

The non-dimensionalized load-displacement response at the center of the footing is shown in Fig. 17, together with the results by GPBEST [Chatterjee (2002)], BEMECH [Gao and Davies (2002)], and ABAQUS (2004). The collapse loads ob-

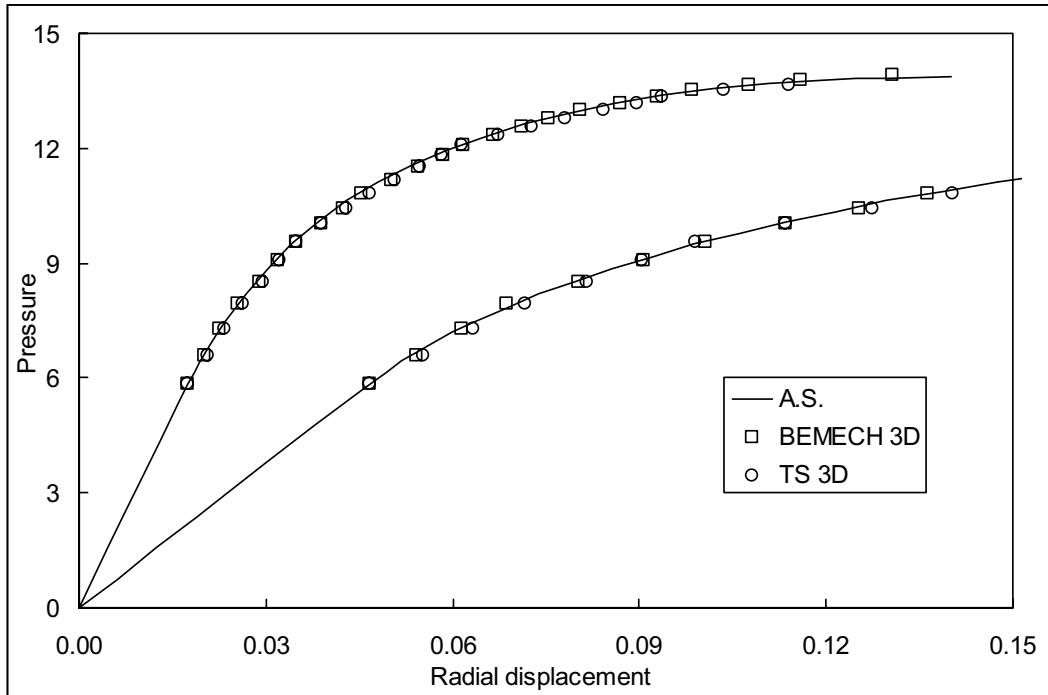


Figure 8: Load-displacement response (Example 3)

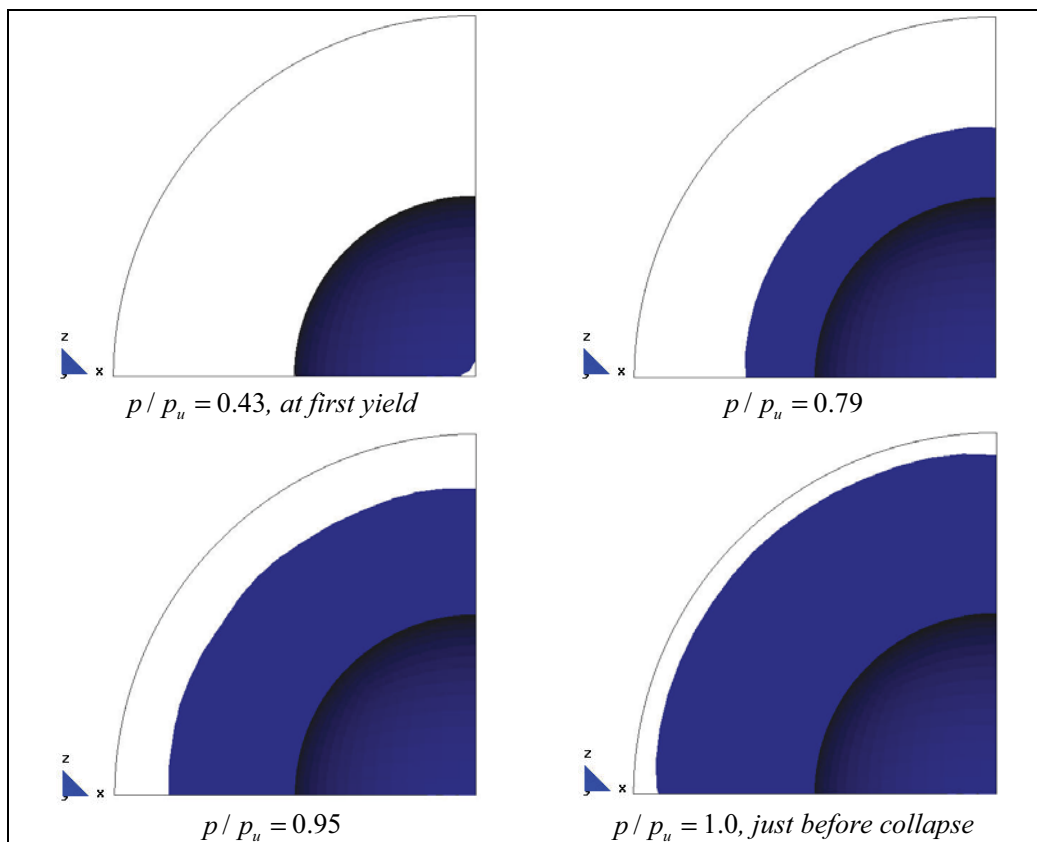


Figure 9: Evolution of plastic region (Example 3)

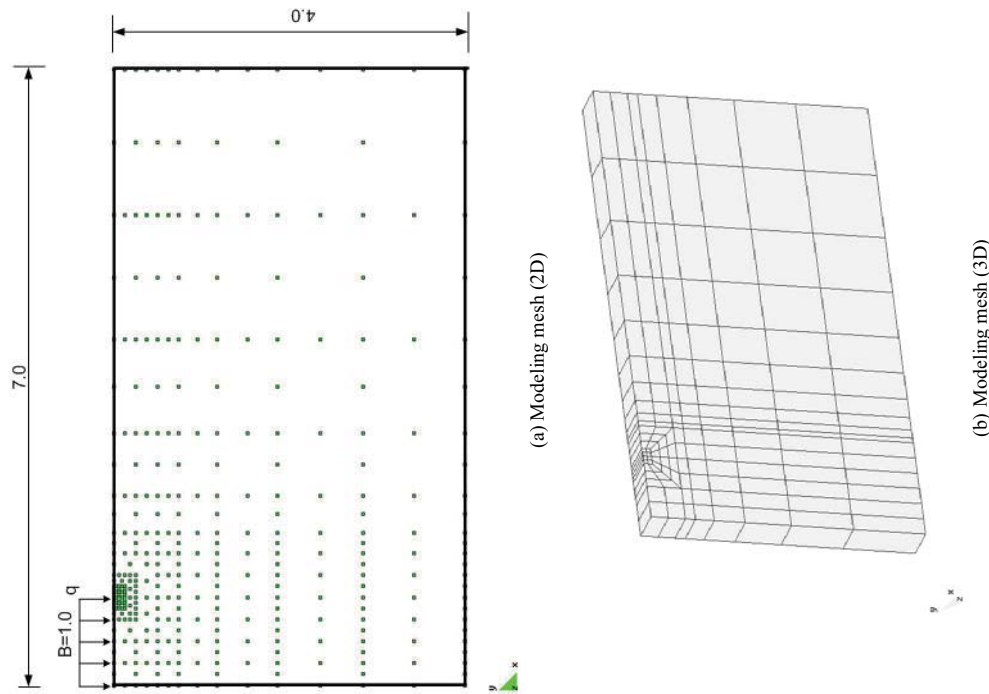


Figure 10: A flexible strip footing (Example 4)

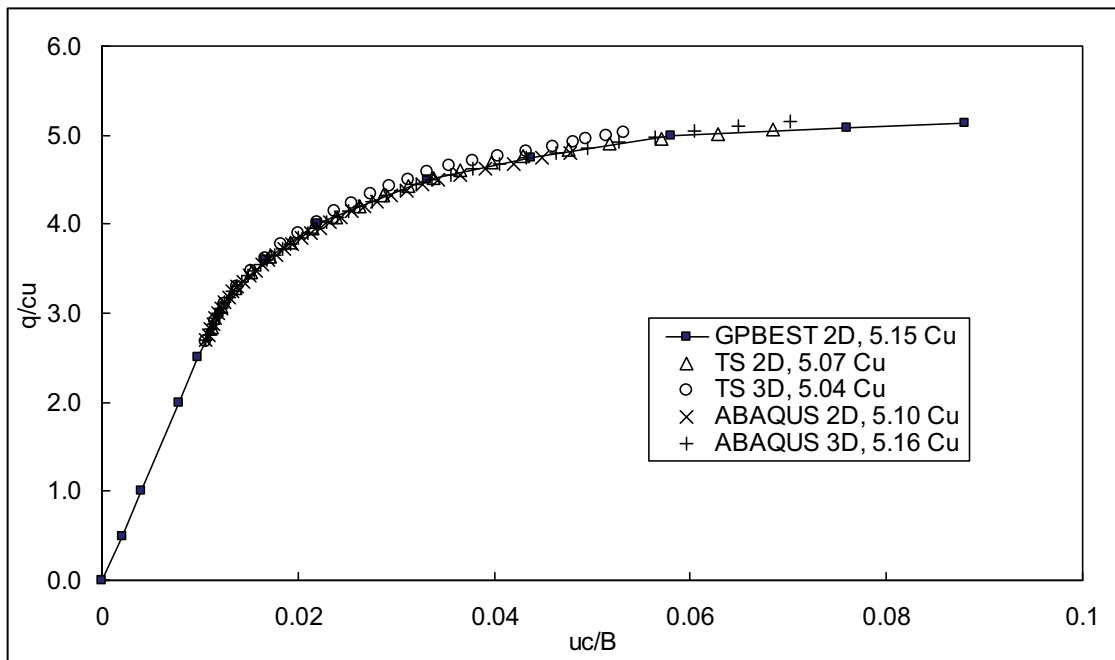


Figure 11: Load-displacement response (Example 4)

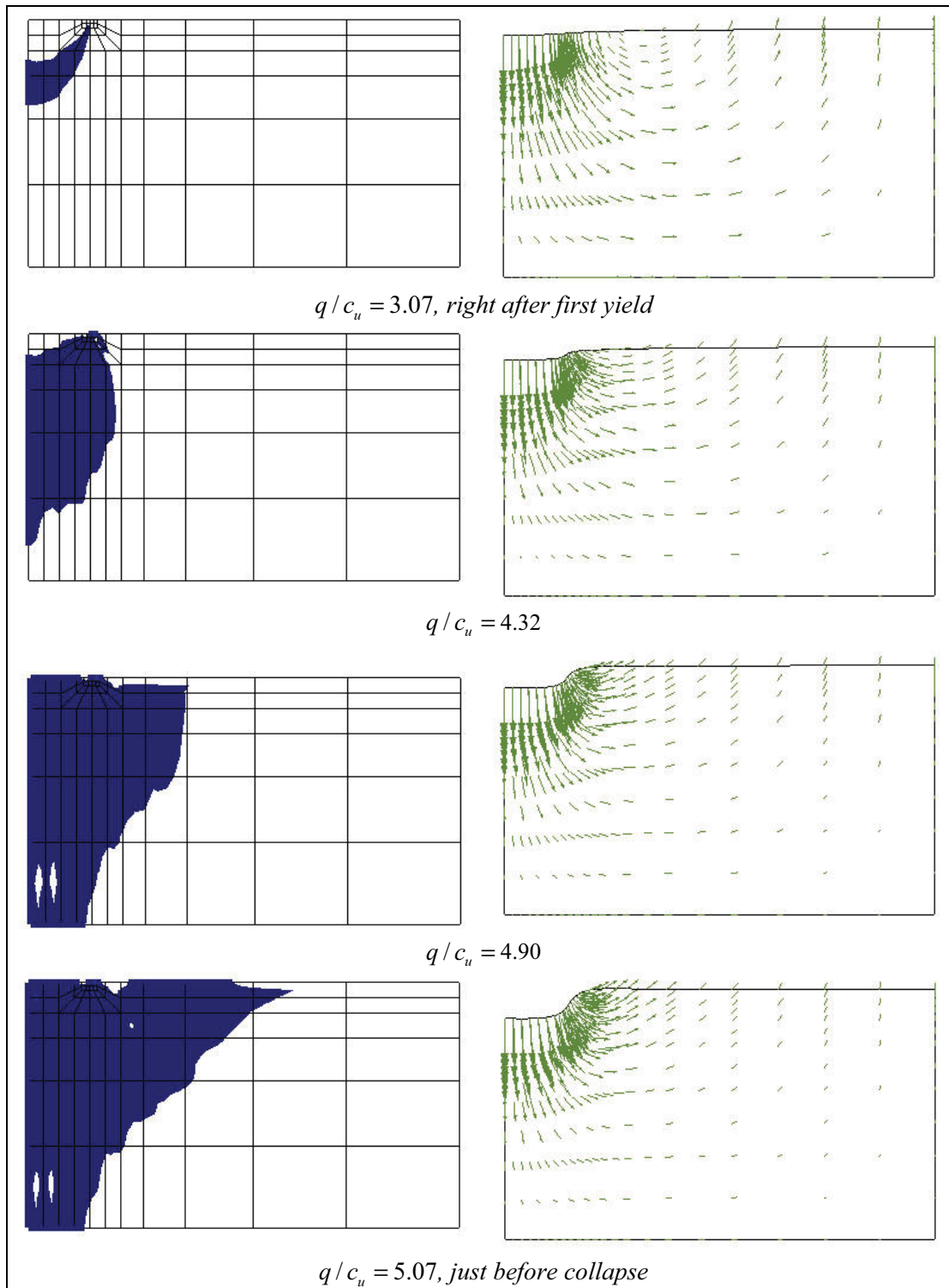


Figure 12: Evolution of plastic region (2D mesh) & deformed shape (Example 4)

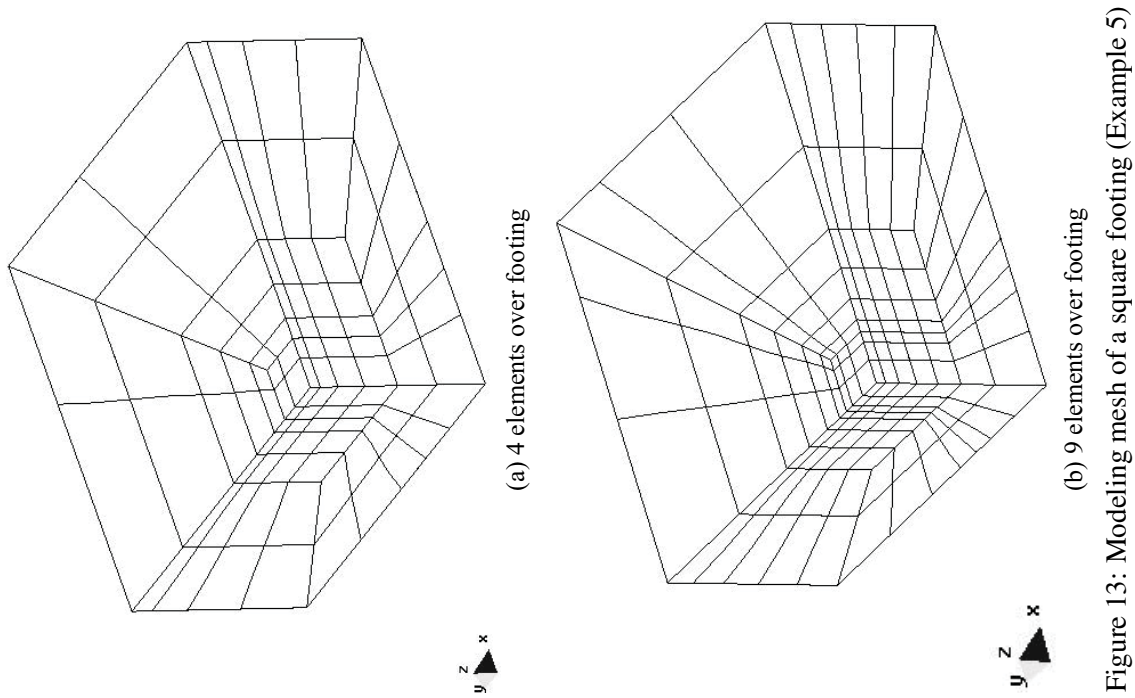


Figure 13: Modeling mesh of a square footing (Example 5)

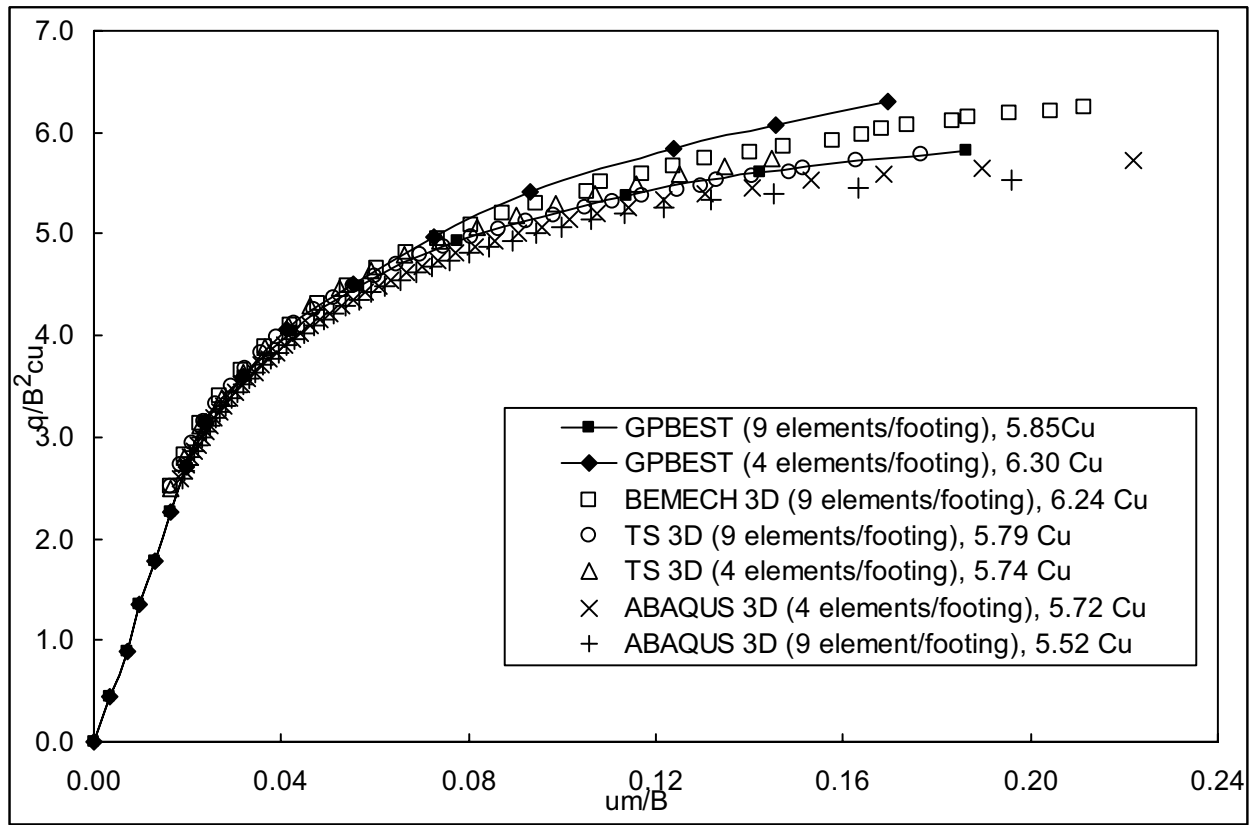


Figure 14: Load-mean displacement response (Example 5)

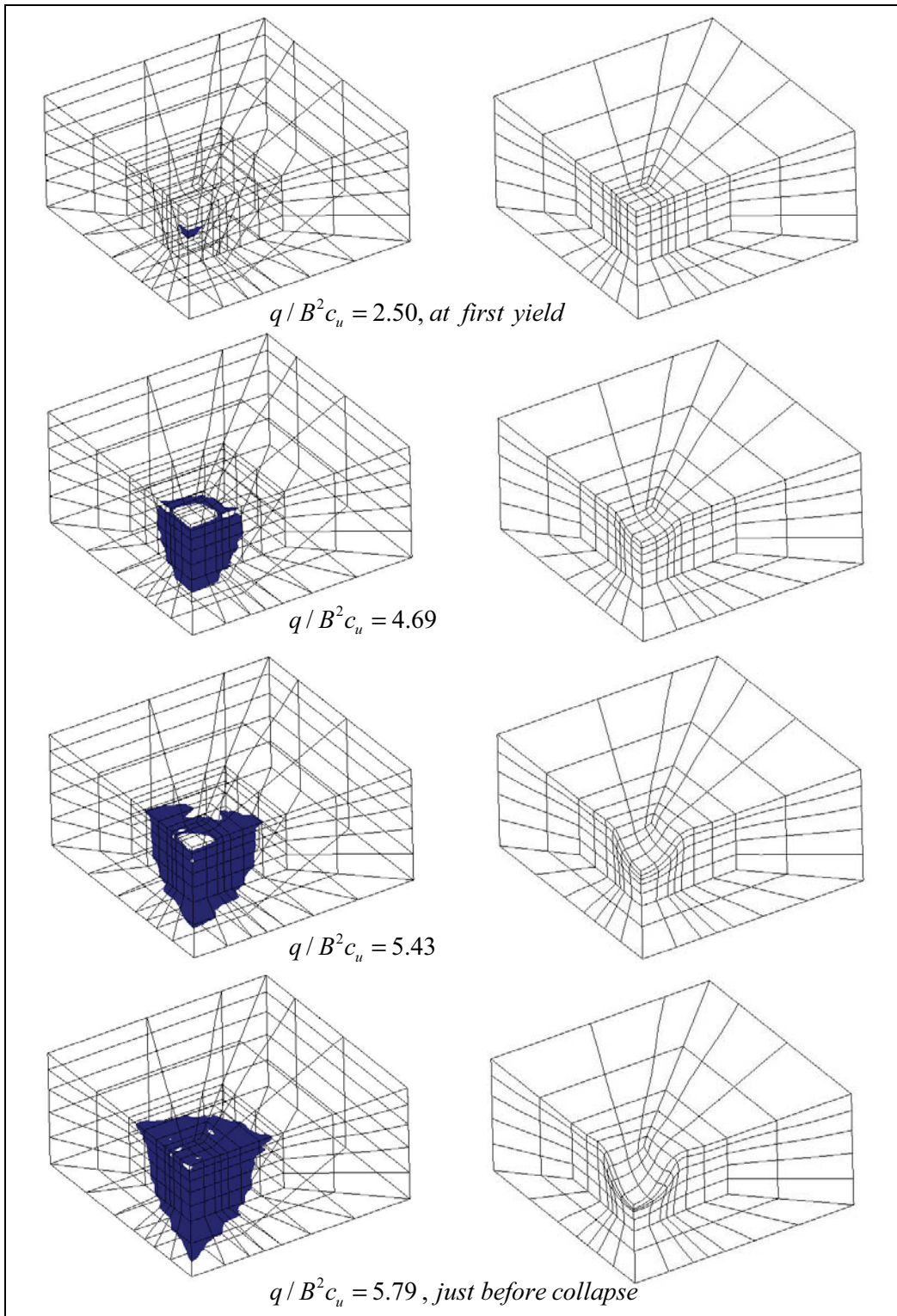


Figure 15: Evolution of plastic region & deformed shape (Example 5)

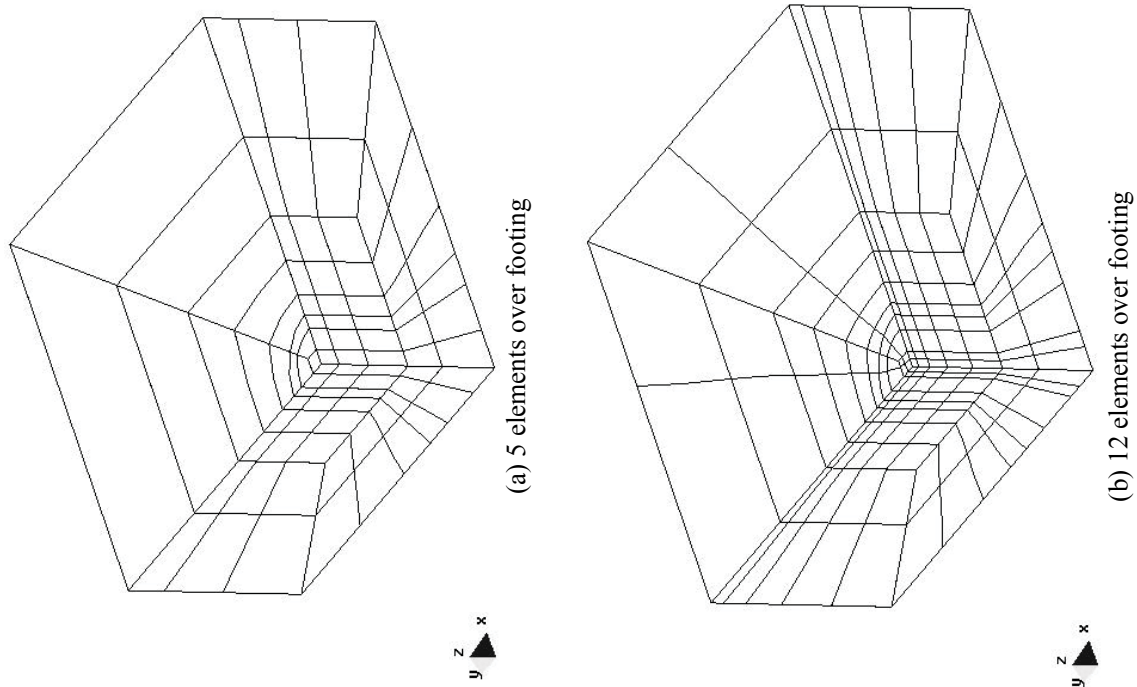


Figure 16: Modeling mesh of a circular footing (Example 6)

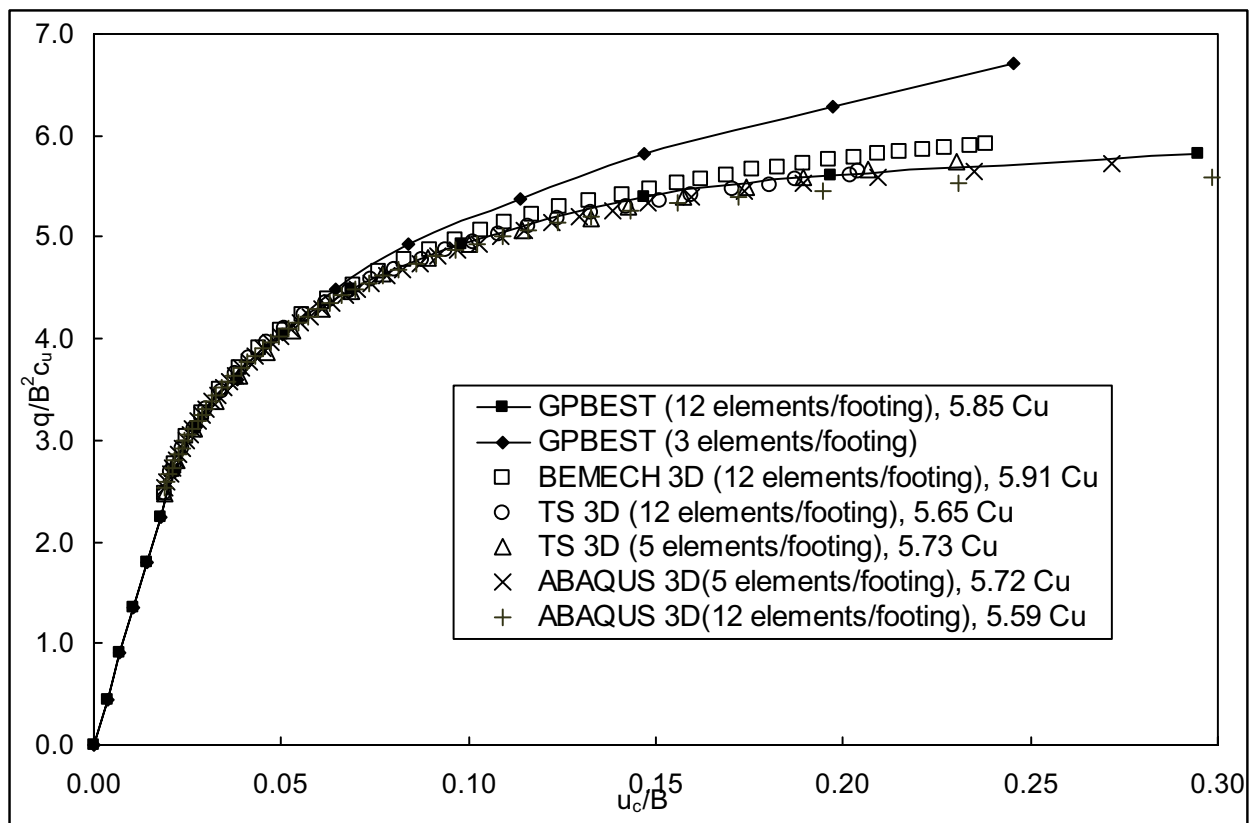


Figure 17: Load-displacement response (Example 6)

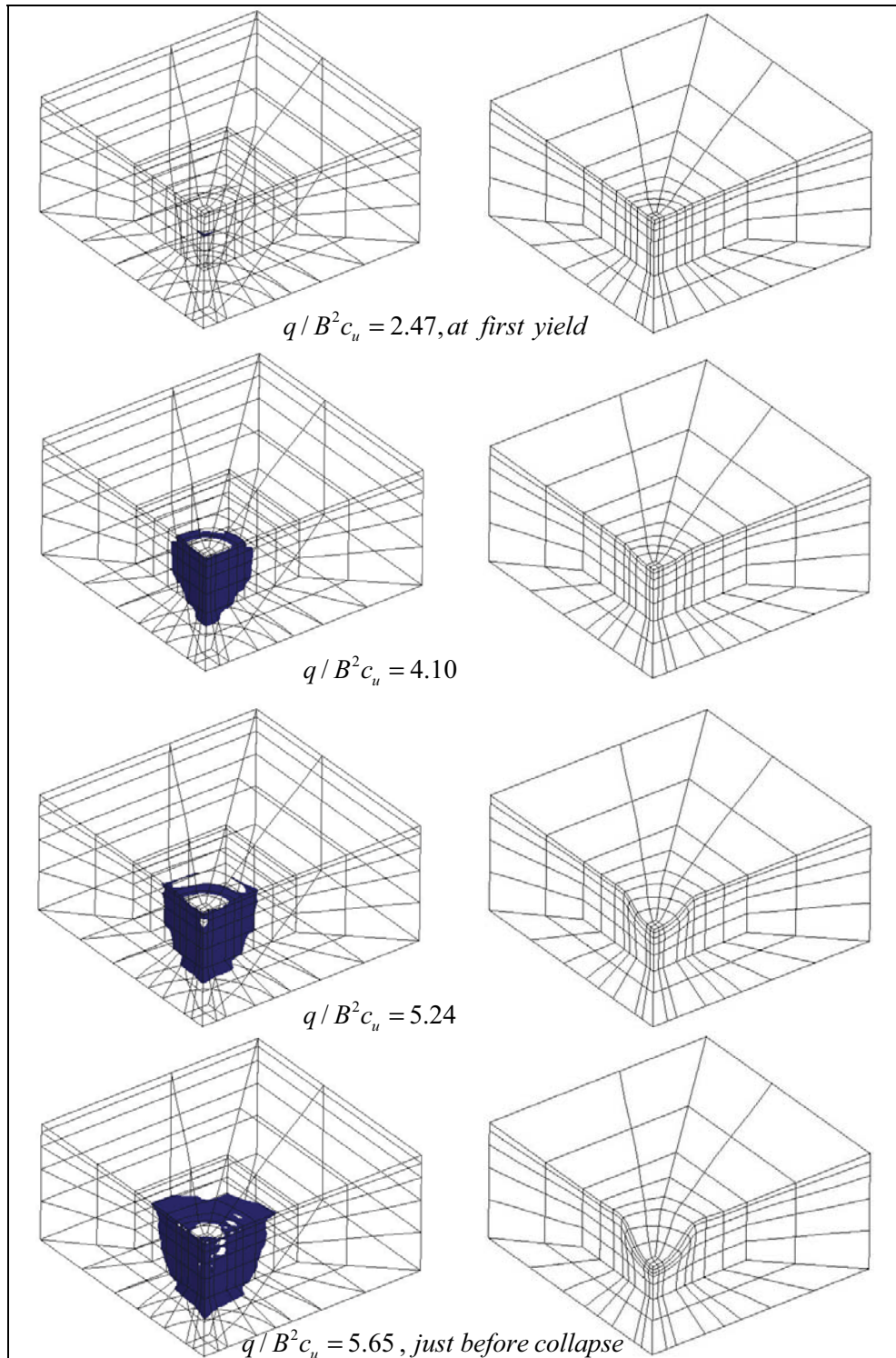


Figure 18: Evolution of plastic region & deformed shape (Example 6)

tained from the present analysis are  $5.73 c_u$  and  $5.65 c_u$  for five and twelve elements over footing respectively, indicating the acceptable accuracy of the formulation using small number of boundary elements and interior points. The development of plastic region and the corresponding deformed shape (2 times magnified) by the load increment, as shown in Fig. 18, demonstrates the validity of the formulation. It can be seen from Figs. 15 and 18 that the expansion pattern of plastic region with increasing load is similar in both of square and circular footings.

## 5 Conclusions

The application of BEM to 2D and 3D elastoplastic analyses has been described by using particular integrals. The elastostatic equation is used for the complementary solution and thus the computer program for the present formulation can be easily implemented from any available program for elastostatic problems by including the Newton-Raphson iterative scheme. The program is integrated with the pre- and post-processor.

The application and accuracy of the present formulation are evaluated by comparing the results of several example problems with their analytical solutions and those by other BEM and FEM programs. It has been demonstrated that 2D and 3D elastoplasticity can be solved using the well-known method of particular integrals.

## References

- ABAQUS Inc.** (2004): ABAQUS 6.5 Documentation.
- Albuquerque, E.L.; Aliabadi, M.H.** (2008): A boundary element formulation for boundary only analysis of thin shallow shells. *CMES: Computer Modeling in Engineering & Sciences*, vol. 29, pp. 63-73.
- Banerjee, P.K.** (1994): *The boundary element methods in engineering*. McGraw-Hill, London.
- Banerjee, P.K.; Butterfield, R.** (1981): *Boundary element methods in engineering science*. McGraw-Hill, London.
- Banerjee, P.K.; Raveendra, S.T.** (1986): Advanced boundary element analysis of two- and three-dimensional problems of elastoplasticity. *International Journal for Numerical Methods in Engineering*, vol. 23, pp. 985-1002.
- Banerjee, P.K.; Raveendra, S.T.** (1987): A new boundary element formulation for two-dimensional elastoplastic analysis. *Journal of Engineering Mechanics ASCE*, vol. 113, pp. 252-265.
- Banerjee, P.K.; Cathie, D.N.; Davies, T.G.** (1979): Two and three-dimensional problems of elasto-plasticity. In: P.K. Banerjee, R. Butterfield (eds.) *Developments in boundary element methods*, Elsevier, Barking, Essex, UK.
- Banallal, A.; Fudoli, C.A.; Venturini, W.S.** (2002): An implicit BEM formulation for gradient plasticity and localization phenomena. *International Journal for Numerical Methods in Engineering*, vol. 53, pp. 1853-1869.
- Bonnet, M.; Mukherjee, S.** (1996): Implicit BEM formulations for usual and sensitivity problems in elastoplasticity using the consistent tangent operator concept. *International Journal of Solids and Structures*, vol.33, pp. 4461-4480.
- Cathie, D.N.; Banerjee, P.K.** (1980): A direct formulation and numerical implementation of the boundary element method for two-dimensional problems of elastoplasticity. *International Journal of Mechanical Science*, vol. 22, pp. 233-245.
- Chandra, A.; Mukherjee, S.** (1996): *Boundary element methods in manufacturing*. Oxford University Press, Oxford, UK.
- Chandra, A.; Saigal, S.** (1991): A boundary element analysis of the axisymmetric extrusion process. *International Journal of Nonlinear Mechanics*, vol. 26, pp. 1-13.
- Chatterjee, J.** (2002): Applications of boundary element method in nonlinear collapse analyses of some footing problems in geomechanics and geotechnical engineering. *MS thesis*, State University of New York at Buffalo.
- Cho, H.A.; Golberg, M.A.; Muleshkov, A.S.; Li, X.** (2004): Trefftz methods for time dependent partial differential equations. *CMC: Computers, Materials, & Continua*, vol. 1, pp. 1-38.

- Chopra, M.B.; Dargush, G.F.** (1994): Development of BEM for thermoplasticity. *International Journal of Solids and Structures*, vol. 31, pp. 1635-1656.
- Cruse, T.A.** (1975): Boundary-integral equation method for 3D elastic fracture mechanics analysis. *AFOSTR-75-0813*.
- Cruse, T.A.; Snow, D.W.; Wilson, R.B.** (1977): Numerical solutions in axisymmetric elasticity. *Computers and Structures*, vol. 7, pp. 445-451.
- Danson, D.J.** (1981): A boundary element formulation of problems in linear isotropic elasticity with body forces. In: C.A. Brebbia (ed), *Boundary Element Methods*, Springer, Berlin.
- Davies, A.J.; Crann, D.; Kane, S.J.; Lai, C.H.** (2007): A hybrid Laplace transform/finite difference boundary element method for diffusion problems. *CMES: Computer Modeling in Engineering & Sciences*, vol. 18, pp. 79-86.
- Dziatkiewicz, G.; Fedelinski, P.** (2007): Dynamic analysis of piezoelectric structures by the dual reciprocity boundary element method. *CMES: Computer Modeling in Engineering & Sciences*, vol. 17, pp. 35-46.
- Fedelinski, P.; Gorski, R.** (2006): Analysis and optimization of dynamically loaded reinforced plates by the coupled boundary and finite element method. *CMES: Computer Modeling in Engineering & Sciences*, vol. 15, pp. 31-40.
- Fung, Y.C.** (1965): *Foundation of solid mechanics*. Prentice-Hall, Englewood, NJ.
- Gao, X.W.** (2002): A boundary element method without internal cells for two-dimensional and three-dimensional elastoplastic problems. *Journal of Applied Mechanics ASME*, vol. 69, pp.154-160.
- Gao, X.W.; Davies, T.G.** (2002): *Boundary element programming in mechanics*, Cambridge University Press.
- GiD.** (2007): *The personal pre and post processor* (ver. 8.0.7). CINME, Barcelona.
- Henry, D.P.; Banerjee, P.K.** (1988): A new BEM formulation for two- and three-dimensional elastoplasticity using particular integrals. *International Journal for Numerical Methods in Engineering*, vol. 26, pp. 2079-2096.
- Hill, R.** (1950): *The mathematical theory of plasticity*, Clarendon Press, Oxford.
- Kogl, M.; Gaul, L.** (2000): A 3-D boundary element method for dynamic analysis of anisotropic elastic solids. *CMES: Computer Modeling in Engineering & Sciences*, vol. 1, pp. 27-43.
- Kumar, V.; Mukherjee, S.** (1977): A boundary integral equation formulation for time dependent inelastic deformation in metals. *International Journal of Mechanical Science*, vol. 19, pp. 713-724.
- Mallardo, V.; Alessandri, C.** (2004): Arc-length procedures with BEM in physically nonlinear problems. *Engineering Analysis with Boundary Elements*, vol. 28, pp. 547-559.
- Mukherjee, S.** (1982): *Boundary elements in creep and fracture*. Applied Science Publishers, London, UK.
- Nardini, D.; Brebbia, C.A.** (1982): A new approach to free-vibration analysis using boundary elements. In: C.A. Brebbia (ed), *Proceedings of the Fourth International Conference on BEM*, Springer, Berlin, pp. 312-326.
- Nardini, D.; Brebbia, C.A.** (1986): Transient boundary element elastodynamics using the dual reciprocity method and modal superposition. In: *Boundary elements VIII*, Computational Mechanics Publications/Springer, Southampton/Berlin, vol. 1, pp. 435-443.
- Ochiai, Y.** (2001): Steady heat conduction analysis in orthotropic bodies by triple-reciprocity BEM. *CMES: Computer Modeling in Engineering & Sciences*, vol. 2, pp. 435-446.
- Ochiai, Y.; Kobayashi, T.** (1999): Initial stress formulation for elastoplastic analysis by improved multi-reciprocity boundary element method. *Engineering Analysis with Boundary Elements*, vol. 23, pp. 167-173.
- Okada, H.; Rajiyah, H.; Atluri, S.N.** (1989): Non-hyper-singular integral-representations for velocity (displacement) gradients in elastic/plastic solids. *Computational Mechanics*, vol. 4(3), pp. 165-175.
- Okada, H.; Rajiyah, H.; Atluri, S.N.** (1990):

A full tangent stiffness field-boundary element formulation for geometric and material nonlinear problems of solid mechanics. *International Journal for Numerical Methods in Engineering*, vol. 29, pp. 15-35.

**Okada, H.; Atluri, S.N.** (1992a): Some recent developments in the field-boundary element method for finite/small strain elastoplasticity. In: P.K. Banerjee (ed), *Nonlinear Problems of Solid Mechanics (Developments in BEM-8)*, Elsevier Science.

**Okada, H.; Atluri, S.N.** (1992b): Field/boundary element method for nonlinear solid mechanics. In: S.N. Atluri (ed), *Nonlinear Computational Mechanics Aerospace Engineering*, AIAA Progress in Aeronautics and Astronautics Series.

**Okada, H.; Atluri, S.N.** (1994): Recent developments in the field-boundary element method for finite/small strain elastoplasticity. *International Journal of Solids and Structures*, vol. 31, pp. 1737-1775.

**Owatsiriwong, A.; Park, K.H.** (2008): A BEM formulation for transient dynamic elastoplastic analysis via particular integrals. *International Journal of Solids and Structures*, vol. 45, pp. 2561-2582.

**Park, K.H.** (2002): A BEM formulation for axisymmetric elasticity with arbitrary body forces using particular integrals. *Computers and Structures*, vol. 80, pp. 2507-2514.

**Park, K.H.** (2003): A BEM formulation for inhomogeneous potential problems by particular integrals. *Applied Mathematical Modelling*, vol. 27, pp. 293-306.

**Park, K.H.; Banerjee, P.K.** (2002a): Two- and three-dimensional soil consolidation by BEM via particular integrals. *Computer Methods in Applied Mechanics and Engineering*, vol. 191, pp. 3233-3255.

**Park, K.H.; Banerjee, P.K.** (2002b): Two- and three-dimensional transient thermoelastic analysis by BEM via particular integrals. *International Journal of Solids and Structures*, vol. 39, pp. 2871-2892.

**Park, K.H.; Banerjee, P.K.** (2006): A simple BEM formulation for poroelasticity via particu-

lar integrals. *International Journal of Solids and Structures*, vol. 43, pp. 3613-3625.

**Park, K.H.; Banerjee, P.K.** (2007): A new BEM formulation for transient axisymmetric poroelasticity via particular integrals. *International Journal of Solids and Structures*, vol. 44, pp. 7276-7290.

**Rizzo, F.J.; Shippy, D.I.** (1977): An advanced boundary integral equation for three-dimensional thermoelasticity. *International Journal for Numerical Methods in Engineering*, vol. 11, pp. 1753-1768.

**Polyzos, D.; Dassios, G.; Beskos, D.E.** (1994): On the equivalence of dual reciprocity and particular integrals approaches in the BEM. *Boundary Element Communications*, vol. 5, pp. 285-288.

**Poon, H.; Mukherjee, S.; Bonnet, M.** (1996): Numerical implementation of a CTO-based implicit approach for the BEM solution of usual and sensitivity problems in elastoplasticity. *Engineering Analysis with Boundary Elements*, vol. 22, pp. 257-269.

**Power, H.; Patridge, P.W.** (1994): The use of Stokes' fundamental solution for the boundary only element formulation of the three-dimensional Navier-Stokes equations for moderate Reynolds numbers. *International Journal for Numerical Methods in Engineering*, vol. 37, pp. 1825-1840.

**Swedlow, J.L.; Cruse, T.A.** (1971): Formulation of boundary integral equations for three-dimensional elastoplastic flow. *International Journal of Solids and Structures*, vol. 7, pp. 1673-1683.

**Telles, J.C.F.** (1983): *The boundary element method applied to inelastic problems*, Springer-Verlag, Berlin.

**Telles, J.C.F.; Brebbia, C.A.** (1979): On the application of the boundary element method to plasticity. *Applied Mathematical Modelling*, vol. 3, pp. 466-470.

**Tsai, C.C.** (2008): Particular solutions of Chebyshev polynomials for polyharmonic and poly-Helmholtz equations. *CMES: Computer Modeling in Engineering & Sciences*, vol. 27, pp. 151-162.

**Wang, C.B.; Chatterjee, J.; Banerjee, P.K.** (2007): An efficient implementation of BEM for two- and three-dimensional multi-region elastoplastic analyses. *Computer Methods in Applied Mechanics and Engineering*, vol. 196, pp. 829-842.

**Wen, P.H.; Aliabadi, M.H.; Young, A.** (2002): Boundary element analysis of curved cracked panels with mechanically fastened repair patches. *CMES: Computer Modeling in Engineering & Sciences*, Vol. 3, pp. 1-10.

**Yang, M.T.; Park, K.H.; Banerjee, P.K.** (2002): 2D and 3D transient heat conduction analysis by BEM via particular integrals. *Computer Methods in Applied Mechanics and Engineering*, vol. 191, pp. 1701-1722.

